International Journal of Pharmaceutics 624 (2022) 121950

Contents lists available at ScienceDirect

International Journal of Pharmaceutics

journal homepage: www.elsevier.com/locate/ijpharm

Soft sensor for content prediction in an integrated continuous pharmaceutical formulation line based on the residence time distribution of unit operations

Martin Gyürkés, Lajos Madarász, Petra Záhonyi, Ákos Köte, Brigitta Nagy, Hajnalka Pataki, Zsombor Kristóf Nagy, András Domokos, Attila Farkas

Department of Organic Chemistry and Technology, Budapest University of Technology and Economics, Műegyetem rkp. 3., H-1111 Budapest, Hungary

ARTICLE INFO

Keywords:
Residence time distribution
Continuous manufacturing
Twin-screw wet granulation
Horizontal fluid bed drying
Oscillating mill
Process modeling

ABSTRACT

In this study, a concentration predicting soft sensor was achieved based on the Residence Time Distribution (RTD) of an integrated, three-step pharmaceutical formulation line. The RTD was investigated with color-based tracer experiments using image analysis. Twin-screw wet granulation (TSWG) was directly coupled with a horizontal fluid bed dryer and an oscillating mill. Based on integrated measurement, we proved that it is also possible to couple the unit operations in silico. Three surrogate tracers were produced with a coloring agent to investigate the separated unit operations and the solid and liquid inputs of the TSWG. The soft sensor's prediction was compared to validating experiments of a 0.05 mg/g (15% of the nominal) concentration change with High-Performance Liquid Chromatography (HPLC) reference measurements of the active ingredient proving the adequacy of the soft sensor (RMSE $< 4\%$).

1. Introduction

The pharmaceutical industry is going through a paradigm shift towards continuous manufacturing (CM). The concept of Quality-by-Design (QbD) and Process Analytical Technology (PAT) framework (FDA, 2004) by the US Food and Drug Administration (FDA) offered an initiative for development, proving that product quality can be achieved without intensive product testing (Juran, 1992). Process understanding gained interest through real-time process monitoring, called PAT tools. Soft sensors and in-line analytical sensors are developed to monitor Critical Quality Attributes (CQAs). Soft sensors predict the Critical Process Parameters (CPPs) from measured attributes of the process (Rehrl et al., 2018). Spectroscopic methods, such as Near Infrared- (NIR) and Raman-spectroscopy, gained increased interest, as non-destructive, fast, in-line analytical tools for solid-state measurements (Adamo et al., 2016, De Beer et al. 2011, 2008, Laske et al., 2017, Simon et al., 2015).

Process monitoring is inevitable in CM (Roggo et al. 2020), because the new time factor. Better process understanding may also overcome the barrier that prevents the industry from developing products with continuous manufacturing. Many research studies present the benefits of CM (Allison et al., 2015, Lee et al., 2015, Plumb, 2005, Poechlauer et al., 2012, Schaber et al., 2011). The authorities (FDA, International Conference on Harmonization (ICH), European Medicines Agency (EMA)) support these steps, as both FDA (2019) and ICH (2016) presented their draft of CM framework.

The CM frameworks emphasize the need for process understanding and the extended role of modeling. The introduction of process dynamics is vital in addressing the challenges of the paradigm shift. Residence Time Distribution (RTD) is the recommended approach to measure and quantify process dynamics (FDA, 2019, ICH, 2016).

RTD is a well-embedded concept for liquids (Nauman, 2008), but due to limited possibilities in solid-state analytical measurements, the concept in solid-state operations is relatively new (Bhalode et al., 2021, Gao et al., 2012a).

The measurement of the RTD requires tracer experiments, preferably impulse disturbances or step disturbances (Bhalode et al., 2021, Gao

Abbreviations: RTD, Residence Time Distribution; CM, Continuous Manufacturing; TSWG, Twin-screw wet granulation; HPLC, High-Performance Liquid Chromatography; NIR, Near Infrared Spectroscopy; QbD, Quality-by-Design; ICH, International Conference on Harmonization; FDA, US Food and Drug Administration; EMA, European Medicines Agency; PAT, Process Analytical Technology; CPP, Critical Process Parameter; CQA, Critical Quality Attribute; CU, Content Uniformity; PDF, Probability Distribution Function; CDF, Cumulative Distribution Function; MRT, Mean Residence Time; PF, Plug flow; CSTR, Continuously Stirred Tank Reactor; TIS, Tank-in-Series; N, Number of tanks; DT, Dead Time; API, Active Pharmaceutical Ingredient; CAR, Carvedilol; L/S, Liquid to Solid Ratio; PTFE, polytetrafluoroethylene; rpm, revolutions per minute; HSV, Hue, Saturation, Value color space; fps, frame per seconds.

https://doi.org/10.1016/j.ijpharm.2022.121950
Received 31 March 2022; Received in revised form 14 June 2022; Accepted 20 June 2022
Available online 23 June 2022

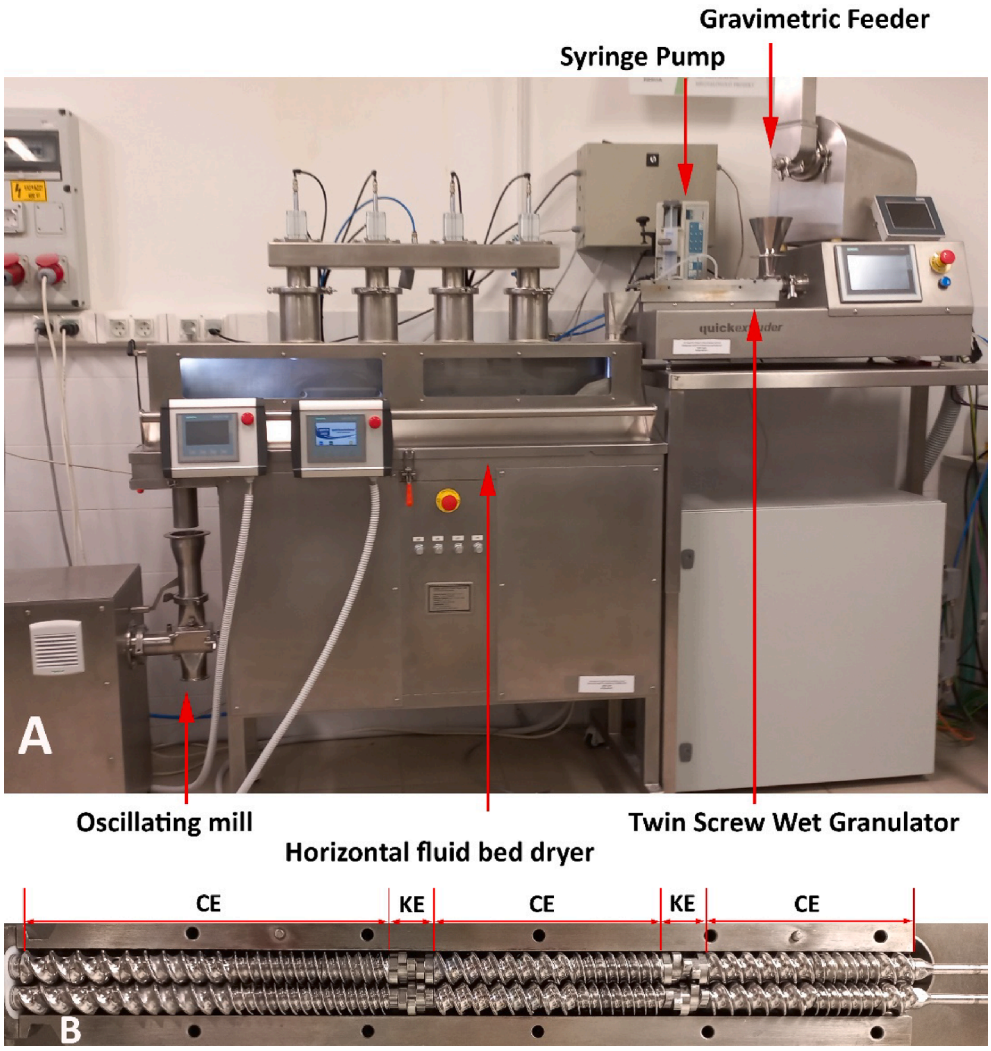

Fig. 1. Investigated pharmaceutical line **a.**, Integrated system of TSWG, horizontal fluid bed dryer and oscillating mill **b.**, Screw configuration of the Twin-Screw Equipment (CE: Conveying Element, KE: Kneading element).

et al., 2012a, Ierapetritou et al., 2018). Impulse disturbance is a straightforward way of measuring RTD, as the Probability Distribution Function (PDF) can be calculated directly from the response function (Ierapetritou et al., 2018). However, in closed systems, step disturbance is easier to measure. The calculation of the RTD is similarly simple, as the Cumulative Distribution Function (CDF) can be calculated from the step response (Ierapetritou et al., 2018). Tank-in-Series (TIS) and Axial Dispersion models are transferred from liquid operations but work for solid operations as well (Bhalode et al., 2021, Gao et al., 2012a, Oka et al., 2018).

While some solid-state operations are inherently continuous (tableting, dry granulation via roller compactors and milling), most batch pharmaceutical unit operations have found their continuous counterparts in recent years. There are examples of RTD measurements for most single unit operations. This includes powder blenders (Beke et al., 2021, Engisch and Muzzio, 2016, Gao et al., 2012b, 2011, Gyürkés et al., 2020, Ierapetritou et al., 2018, Muzzio and Oka, 2017, Oka et al., 2018), roller compactors (Kruisz et al., 2017), wet granulators (Kotamarthy and Ramachandran, 2021, Kumar et al., 2016, 2015, Plath et al., 2021, Rahimi et al., 2020), extruders (Wahl et al., 2018, Wesholowski et al., 2019, 2018), tableting feed-frames (Dülle et al., 2018, Furukawa et al., 2020, Tanimura et al., 2021), dryers (Babu and Setty, 2003, Chen et al., 2020) and mills (Mangal and Kleinebudde, 2017).

However, only a few examples present the investigation of integrated processes. The two-step process of directly compressed tablets was published by Tian et al. (2021) and Karttunen et al. (2020). Tian et al. (2021) presented an RTD-based modeling framework with gPROMS. Karttunen et al. (2020) investigated the robustness of the direct compression system based on the RTD, measured with two NIR probes, where the disturbances were introduced to the blender and measured after the blender and after the tablet press. A three-step dry granulation process was investigated by Martinetz et al. (2018), measuring the change of RTD by monitoring the process stream at three points with NIR probes during step changes. Finally, Karttunen et al. (2019) investigated three continuous manufacturing lines: hot-melt extrusion line, dry granulation line and wet granulation line. The unit operations were separated for the measurement and the integrated process was only presented with the in silico convolution of the measured RTDs. The convolution-based coupling of consecutive unit operations is described by Engisch and Muzzio (2016) and used as an assumption by Martinetz et al. and Karttunen et al., but the separated and the integrated system has not been experimentally compared before.

The Q13 guideline focuses on the integrated aspect of CM where unit operations are coupled in a continuous manner (ICH, 2016). End-to-end product lines were developed using only continuous manufacturing with different products (Adamo et al., 2016, Balogh et al., 2018, Cole et al., 2017, Mascia et al., 2013). A proof of concept end-to-end CM line was recently published for producing traditional tablet form (Domokos et al.,

2020). Integrated technologies amplify the advantages of CM (Bhaskar and Singh, 2019, Domokos et al., 2021a), but also provide numerous new challenges (Domokos et al., 2021a), mostly through the increased number of CPPs.

Most pharmaceutical technologies include wet granulation to address flowability problems, but wet granulation must be immediately followed by drying and regranulation. Therefore, this technology requires integration of the unit operations. Twin-screw wet granulation (TSWG) is a thoroughly investigated continuous form of wet granulation (Kumar et al., 2016). In most cases, continuous drying is operated semi-continuously with segmented fluid bed dryers (Pauli et al., 2020, Silva et al., 2018). Still, horizontal fluid bed drying may be a new continuous alternative to be applied in pharmaceutical processes, where the materials are transported via vibration of a perforated belt, and the granules are dried by airflow through the bed (Domokos et al., 2021b, 2020, Fülöp et al., 2021).

In this paper, an integrated system of the three essential unit operations of the powder to granule pharmaceutical formulation line (Fülöp et al., 2021, Kreimer et al., 2018) was investigated, with extremely low API content in the granulation liquid, considering the process dynamics of the system. The concept maximizes the process knowledge by separating the unit operations and exploring the feasibility of integrating models in silico. Furthermore, a concentration predicting soft sensor was developed based on the process dynamics to address real-time content uniformity, even in extremely low concentrations. The process was examined through four tracer inputs, as the powder blend and the granulation liquid are separated in the TSWG process, and the dryer and mill are investigated with premade granules. RTD was measured with in-line high-speed process camera with coloring agent-based tracers. According to the authors' knowledge, RTD of a horizontal fluid bed dryer and an integrated three-step pharmaceutical process was not investigated before.

2. Materials and methods

2.1. Materials

Carvedilol (CAR, Sigma-Aldrich, Budapest, Hungary) with a purity of $\geq$ 98 % and a melting point of 117 °C was selected as a model active pharmaceutical ingredient (API). The API was dissolved in 96% ethanol (Sigma-Aldrich, Budapest, Hungary) along with Kollidon® 30 (Povidon, PVPK30, BASF, Ludwigshafen, Germany). Fine α-lactose monohydrate (GranuLac® 230 mesh, Meggle Pharma, Wasserburg, Germany) and potato starch (Roquette Pharma, Lestrem, France) were used as the solid excipients for the granulation.

Blue coloring agent (Brilliant Blue R, Sigma-Aldrich, Budapest, Hungary) was used as a tracer in the granulation liquid and in the powder blend.

2.2. Granulation

The integrated system is presented in Fig. 1 a. Twin-Screw Wet Granulation (TSWG) was carried out in a continuous manner in a multifunctional continuous twin-screw equipment (TS16, Quick 2000 Ltd., Hungary) with a screw diameter of 16 mm (25 L/D ratio), and a configuration that contained conveying elements (CE) and kneading elements (KE) (Fig. 1 b). No heating was applied during the TSWG experiments. The multifunctional continuous twin-screw equipment was directly connected to the dryer's hopper.

The lactose and the potato starch were pre-blended manually for 5 min to eliminate the possible error coming from the improper blending (in the TSWG) or feeding of the two materials. The pre-blend was fed with a gravimetric feeder (type: DDW-MD0-MT HYD ISC plus, Brabender Technologie, Duisburg, Germany).

The API and the PVPK30 were dissolved in ethanol and stirred for 24 h with a magnetic stirrer to provide the granulation liquid. This liquid was dosed into the second zone of the granulator with a syringe pump (SEP-10S Plus, Aitecs, Vilnius, Lithuania) through a silicone tube with an inner diameter of 3.1 mm.

During the experiments, the feeding rates were set either to 1.0 kg/h solid feeding or to 1.5 kg/h solid feeding on the gravimetric feeder. The feeding of the ethanol solution was changed accordingly, keeping a constant liquid-to-solid ratio (L/S) of 0.14 with a target concentration of 0.35 mg/g for CAR. The screw rotation speed was set between 200 and 400 rpm (revolutions per minute) in the experiments.

2.3. Drying and milling

Drying of the granules was conducted in a continuous horizontal fluid bed dryer (Quick 2000 Ltd., Hungary). The material was transported by the vibration of 50 Hz frequency.

The dryer consisted of four drying zones with independent airflow and a 0.024 m^2/zone surface area. The airflow was varied between 60 L/min and 120 L/min in the experiments, always using even flow in the four zones, and the air temperature of the first three zones was set to 30 °C. The last zone was not heated, as it was used for the conditioning of the granules. Each zone had its corresponding filter bag automatically dedusted every 2 min. Perforated conveyor was applied to enable the passing of the supply air.

The dried granules were directly transported into the continuous mill (Quick 2000 Ltd., Hungary). The mill was used in oscillating mode with a sieve size of 1.5 mm, where large agglomerates were broken down. The oscillation intensity was investigated as the CPP of the mill and was varied between 100 oscillations per minute to 200 oscillations per minute for the experiments.

2.4. Tracer experiments

Color-based tracer experiments were executed to measure the RTD of each process step, then a step change validation experiment was carried out with the whole integrated system by changing the liquid feeding rate.

Three colored tracers were produced as surrogate materials to examine different unit operations.

First, a colored powder blend was produced by blending the original powder blend of lactose and potato starch with an additional 1 w/w% of the blue coloring agent.

Then, colored granulation liquid was produced by stirring 1 w/w% blue coloring agent to the granulation liquid.

Finally, colored granules were produced by wet granulation of the original powder blend and the colored granulation liquid. The granules were dried and collected without milling to provide a trace material with similar particle size distribution as of the produced non-colored granules.

The colored granulation liquid was used during step change experiments of the liquid phase of the TSWG process. Two identical syringe pumps were used, with the original granulation liquid and with the colored one. At the start of the measurement, the silicone tubes of the pumps have been replaced on the nozzle; that is, instead of the original liquid, the colored one was introduced. This change caused a negligible disturbance in the liquid flow.

Solid material flows were measured with impulse disturbances by adding a certain amount of solid tracer into the hopper. In the case of TSWG 0.2 g of the colored powder blend was used as a tracer, while for the dryer and the mill, 1.0 g of the colored granules were used. The amount of tracer was minimized for every process during preliminary experiments to achieve minimal disturbance compared to the mass hold-up while maintaining reliable responses.

In each unit operation, we used the same camera setup involving an RGB process camera (Basler acA4112-30uc) and a ring light consisting of 114 LEDs (Apokromat Ltd, Hungary), which provided homogenous illumination for the particles. A custom slope has been designed and 3D

printed for each unit operation in order to guide the produced particles into a single plane.

During the experiments, the camera was operated at 30 frame per seconds (FPS). As the Value dimension of the HSV color space (Hue, Saturation, Value) corresponded the most with the change in the color of the produced material, this color space was used during image analysis investigations. Each recording was started simultaneously with the disturbance. The recorded videos were analyzed with an image analysis software developed by the authors (Videometry).

2.5. Validating measurement

The models were used as a soft sensor for API prediction by means of the surrogate tracer. The soft sensor was validated by following the API concentration during two experiments by High-Performance Liquid Chromatography (HPLC) and the results were compared with the prediction.

The granulation liquid contained a very low amount of CAR, therefore, direct monitoring of its concentration was unachievable by in-line spectroscopic methods, and soft sensors are required. To reduce the impact of the disturbance, we raised the liquid flow by 15% to make a step disturbance and a short step disturbance, where the disturbance was terminated before the system settled in stationary state. In the case of short step disturbance, the liquid flow was restored after 1 min.

The product was sampled after the mill. One sample was taken before the disturbance as the zero point. Continuous sampling was done after 50 s by collecting the product every 10 s for the duration of 4 s in separate containers. HPLC was applied to measure 100 mg of each collected granule. The samples were weighed into 10 mL volumetric flasks, and then they were disintegrated in a mixture of methanol and purified water (1:1) within an ultrasonic bath in 15 min. Upon completion, the suspensions were filtered by a 0.45 μm polytetrafluoroethylene (PTFE) syringe filter. The examinations were carried out on a reversed-phase HPLC column (Agilent 1200 series LC system, Santa Clara, CA, USA) with a gradient elution of 0.1 M phosphoric acid and acetonitrile at 25 °C (flow rate was set to 1.0 mL/min). The concentration of CAR was determined based on the UV absorption of the injected solution at 285 nm. A linear relationship is assumed between the signal/peak area in the chromatogram and the CAR concentration. Single-point calibration was performed to determine the sensitivity of the HPLC-UV method as follows. First, 40 mg CAR was dissolved in methanol and diluted with MeOH:H_2O (1:1) in a volumetric flask to 4 μg/ml. Then 1 mL solution was injected. The measurement was replicated four times; the calculated mean slope was 51.76 ± 1.58. Because of the low CAR content, the measurement is challenging, as the resolution of the method corresponds to a 3% relative error for concentration.

2.6. Residence time Distribution

Tracer experiments were used to model Residence Time Distribution. Impulse and step responses were calculated from the color change during impulse and step disturbances. In the case of impulse disturbances, the responses were normalized by the area under the curve, according to Eq. (1), while for the step changes the responses were normalized by dividing with the average at the maximum (after the change), according to Eq. (2). The baseline was subtracted in both cases.

$$e(t) = \frac{c_{imp}(t) - c_{imp}(0)}{\int_{t'=0}^{\infty} c_{imp}(t') - c_{imp}(0)dt} \quad (1)$$

$$f(t) = \frac{c_{step}(t) - c_{step}(0)}{c_{step}(\infty) - c_{step}(0)} \quad (2)$$

Where,
e(t) is the measured PDF,
t is the time in seconds,
$c_{imp}(t)$ is the measured response for impulse disturbances at t timepoint,
f(t) is the measured CDF,
$c_{step}(t)$ is the measured response for step disturbances at t timepoint.

Two model types were used to model RTD. Three parametric TIS was calculated according to Eq. (3)–(4). The model used the Mean Residence Time (MRT), the number of tanks (N), and the dead time or plug flow (PF) region as the three parameters.

Fokker-Planck based three parametric axial dispersion (Eq. (5)) model combined with PF effect was compared with the TIS model. The Axial Dispersion model used the Mean Residence Time (MRT), the dimensionless Péclet number (Pe), and the dead time or plug flow (PF) region as the three parameters.

Impulse responses were modeled with the PDF, while CDF was used for step responses. CDF was calculated as the numerical integral of the PDF curves (Eq. (6)).

$$E(t) = \frac{N \cdot e^{-\frac{t-t_D}{\tau_{Tank}}} \cdot \left(\frac{t-t_D}{\tau_{Tank}}\right)^{N-1}}{(\tau_{TIS} - t_D) \cdot (N-1)!} \quad (3)$$

$$\tau_{Tank} = \frac{\tau_{TIS} - t_D}{N} \quad (4)$$

Where,
E(t) is the PDF based on TIS model,
t is the time in seconds,
N is the number of tanks in the model,
t_D is the dead time in seconds, corresponding to the PF region,
τ_{Tank} is the mean residence time for each tank in the model,
τ_{TIS} is the mean residence time for the model.

$$E(t) = \sqrt{\frac{Pe}{4\pi\left(\frac{t-t_D}{\tau-t_D}\right)}} \cdot Exp\left[-\frac{Pe \cdot \left(1 - \frac{t-t_D}{\tau-t_D}\right)^2}{4 \cdot \frac{t-t_D}{\tau-t_D}}\right] \quad (5)$$

Where,
E(t) is the PDF based on AD model,
t is the time in seconds,
Pe is the dimensionless Péclet number,
t_D is the dead time in seconds, corresponding to the PF region,
τ is the mean residence time for the model.

$$F(t) = \int E(t')dt \quad (6)$$

Where,
F(t) is the CDF,
E(t) is the PDF.

Modeling was done with Least Squares modeling in Matlab, based on Eq. (7). Axial dispersion and TIS models were developed for each experiment, and the best models were chosen for each unit operation.

$$SSE = \sum_{i=1}^{n} [G(t_i) - g(i)]^2 \quad (7)$$

Where,
SSE is the sum of square error,
n is the number of measurements,
G(t) is the model curve at t timepoint,
t_i is the timepoint corresponding to the i-th measurement,
g(i) is the measured curve at the i-th measurement point.

3. Results and discussion

3.1. RTD measurement of the Twin-screw wet granulator

The TSWG has two different inputs, the powder blend and the granulation liquid. The two inputs significantly differ in their physical

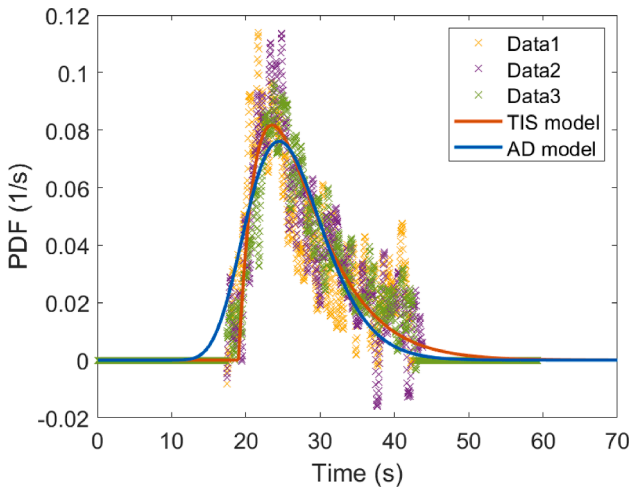

Fig. 2. Model fit for powder impulse in the TSWG process.

attributes as well as the location of the input ports. Therefore, independent measurements were required.

The powder mixture is fed into the hopper of the granulator. In the first segment of the granulator, the powder is transported and blended by the screws. The screws in this region only contain conveying elements. This section is essential, and it works as a buffer for the imperfections during blending and powder feeding.

In the next segment of the granulator, the granulation liquid is fed through a nozzle by a syringe pump. The screws, starting from this section contain conveying and kneading zones, where the powder blend and the granulation liquid could be mixed and the granules are formed.

The RTD of the TSWG apparatus relying on these two inputs was measured independently, using the colored powder blend and the colored granulation liquid. The same experimental design with two factors was used for each material input, testing the effect of mass flow and screw rotation speed. The mass flow was measured on two levels, 1.0 kg/h at the lower level, and 1.5 kg/h at the higher level. Screw rotation speed was tested on 3 levels, 200 rpm at the low level, 300 rpm for the center, and 400 rpm at the high level of the experimental design. Each setting was measured in triplicate.

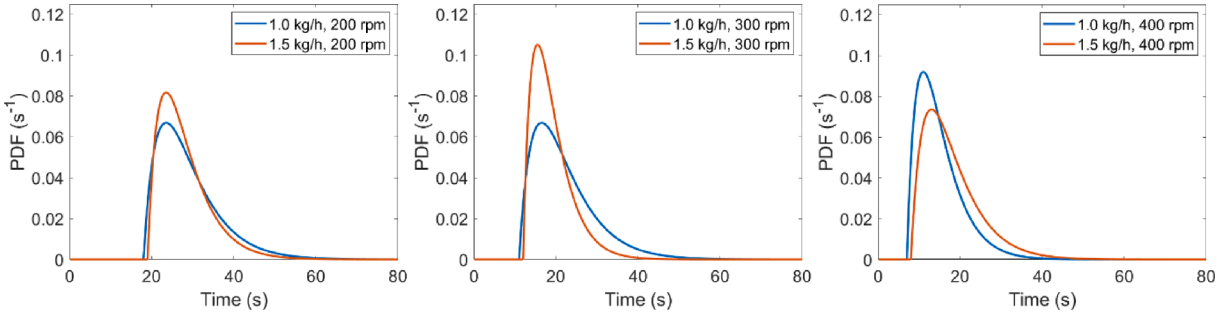

Fig. 3. Effect of mass flow on the RTD of the powder blend in the TSWG process with the TIS models.

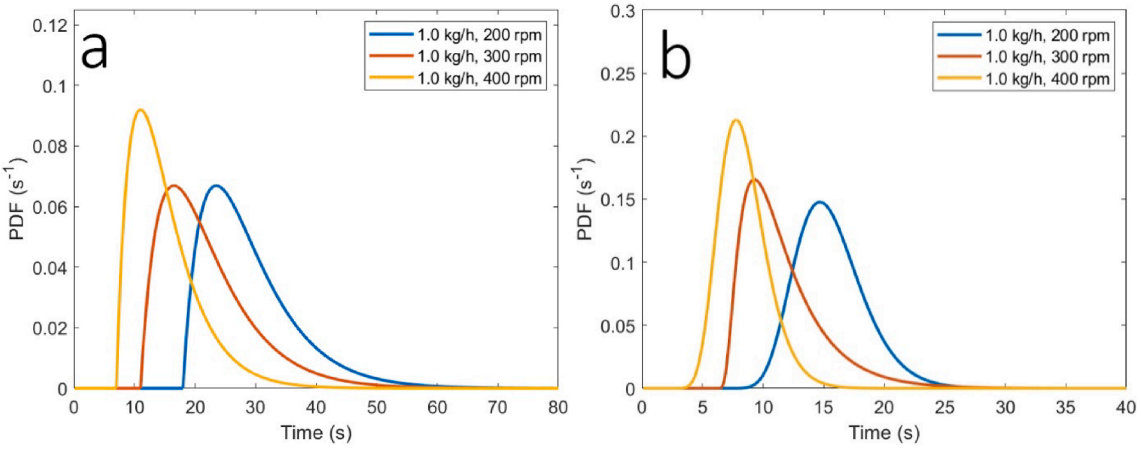

Fig. 4. Effect of screw rotational speed on the RTD of the TSWG. **a.**, Powder blend, constant mass flow, different screw rotation speed with TIS models. **b.**, Granulation liquid, constant mass flow, different screw rotation speed with axial dispersion models.

Table 1
Model parameters of best fitting TIS models during powder blend impulse disturbances and Axial Dispersion models during granulation liquid step disturbances.

Mass flow [kg/h]	Powder blend						Granulation liquid					
	1.0			1.5			1.0			1.5		
Screw Rotation Speed [rpm]	MRT [s]	N [#]	DT [s]	MRT [s]	N [#]	DT [s]	MRT [s]	Pe [-]	DT [s]	MRT [s]	Pe [-]	DT [s]
200	29	2	18	28	2	19	15	39	3	15	13	7
300	22	2	11	19	2	12	10	5	6	8	14	2
400	15	2	7	18	2	8	8	36	0	7	47	0

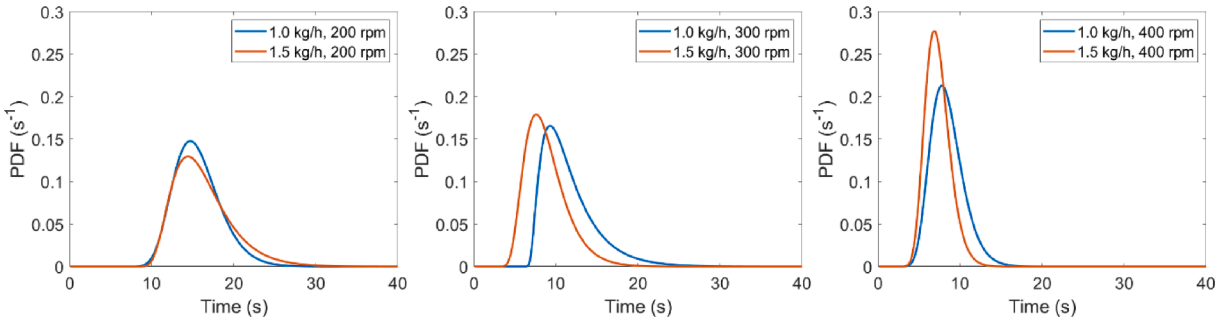

Fig. 5. Effect of mass flow on the RTD of the granulation liquid in the TSWG process with axial dispersion models.

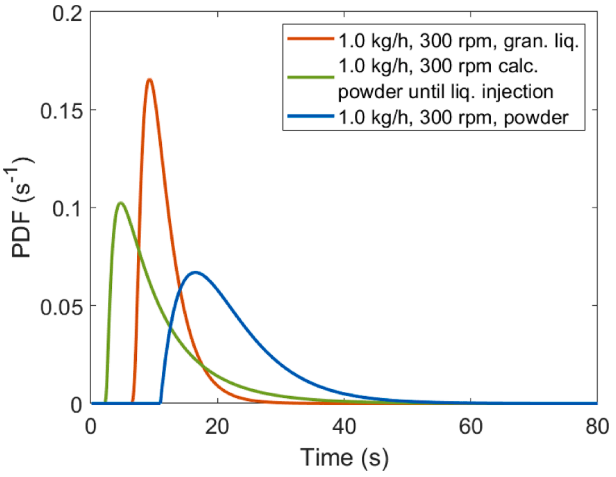

Fig. 6. Difference between granulation liquid and powder RTD. PDF of the granulation liquid (orange) and its difference (green) between powder PDF (blue). (For interpretation of the references to color in this figure legend, the reader is referred to the web version of this article.)

The best models for the impulse responses of the powder blend were achieved with the TIS models, but the axial dispersion models gave similar results (Fig. 2, Supplementary Table 1). As Fig. 3 shows the fitted models, the mass flow had no significant effect on the RTD, but a slight narrowing can be observed as the mass flow increases, while the increase in screw rotation speed lowers the MRT of the system (Fig. 4, Supplementary Table 2). Table 1 summarizes the model parameters.

Axial Dispersion models with three parameters had a slightly better fit for the step responses of colored granulation liquid (Supplementary Fig. 1a, Supplementary Table 1). Similarly to the powder blend, only screw rotation speed affected significantly the RTD (Fig. 4), inversely proportionally to the MRT. The narrowing effect of the mass flow change is even slighter (Fig. 5, Supplementary Table 2).

The MRT of the powder RTD is in the range of 15 s to 30 s. At the same time, the $\sigma_{RTD,TSWG,powder}$, which correlates with the RTD width, is between 5 s and 10 s. The RTD of the granulation liquid is shorter (MRT = 7 s to 15 s) and narrower ($\sigma_{RTD,TSWG,liquid}$ = 1.5 s to 3.5 s).

The granulation liquid and the powder blend mix into a wet blend after the injection of the liquid, and the mix is transported simultaneously. With the assumption of instantaneous mixing, the RTD of the powder blend after the injection equals the RTD of the granulation liquid. In this case, the RTD of the powder blend until the injection can be calculated from the powder blend RTD and the granulation liquid RTD via deconvolution. Fig. 6 shows the result of the deconvolution (green), the PDF of the granulation liquid (orange), and the PDF measured with powder impulse (blue). Generally, the PDF of the granulation liquid is narrower, having a longer dead-time than the calculated powder PDF. Therefore, more mixing occurs before the injection of the granulation liquid rather than after.

Table 2
Model *parameters during the drying experiment design.*

Air flow [L/min]	Mass flow [kg/h]					
	1.0			1.5		
	MRT [s]	N [#]	DT [s]	MRT [s]	N [#]	DT [s]
60	108	89	0	100	5	81
120	81	124	0	87	128	0

3.2. Dryer

The dryer was studied with impulses of colored granules. The TSWG was operated with 400 rpm screw rotational speed. Meanwhile, the mass flow and the drying airflow as the two CPPs were investigated on two levels. According to the experimental design, the powder mass flow was changed from 1.0 kg/h to 1.5 kg/h. The airflow was set at 60 L/min on the lower, and 120 L/min on the higher level.

Our model fitting shows that there is no significant difference between the TIS and axial dispersion model, but TIS models describe the impulse responses more precisely (Supplementary Fig. 1b, Supplementary Table 1). Table 2 presents the parameters of the best fitting models. In most cases, except 1.5 kg/h; 60 L/min, models containing a high number of tanks without dead time had the best fit, where the high number of tanks describes the plug flow region of the RTD, while providing symmetrical curves. According to Fig. 7, the mass flow does not change the RTD significantly. On the contrary, the increased airflow reduces the MRT in the dryer (Supplementary Table 2).

The dryer had a significantly higher MRT (80 s to 110 s) compared to the TSWG. The $\sigma_{RTD,\ dryer}$ (7.2 s to 8.5 s) is comparable with the powder RTD during TSWG.

3.3. Regranulation

Impulse disturbances with colored granules were measured during milling. The mass flow was set to 1.0 kg/h and 1.5 kg/h. The mill was operated with oscillation speeds of 100 min^{-1} and 200 min^{-1} at the lower and higher levels.

Impulse responses had an exponential course similar to the continuously stirred tank reactor (CSTR) models (TIS models with 1 tank). Therefore, TIS models were selected to describe the RTD (Supplementary Fig. 1c, Supplementary Table 1). Table 3 contains the model parameters for the regranulation. The models are very similar (Fig. 8), as we found that the CPPs had no significant effect on the RTD (Supplementary Table 2).

Regranulation has the broadest distribution with σ_{RTD} of 6 s to 15 s, although most of the granules leave the equipment immediately.

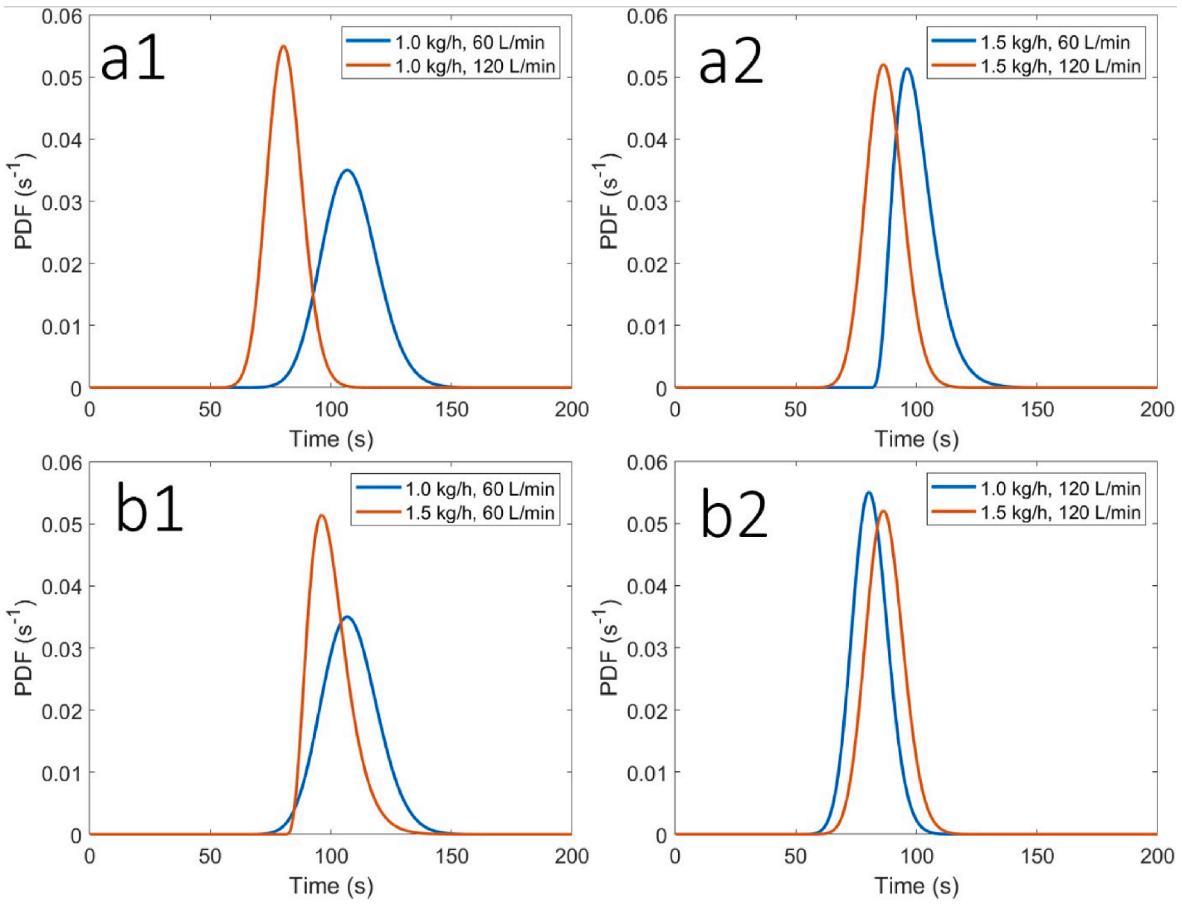

Fig. 7. Effect of CPPs on the RTD of the dryer with TIS models**a.**, Constant mass flow ($\mathbf{a_1}$: 1.0 kg/h; $\mathbf{a_2}$: 1.5 kg/h) **b.**, Constant airflow ($\mathbf{b_1}$: 60 L/min; $\mathbf{b_2}$: 120 L/min).

Table 3
Model *parameters during the milling experiment design.*

Oscillation speed [min^{-1}]	Mass flow [kg/h]	1.0			1.5		
		MRT [s]	N [#]	DT [s]	MRT [s]	N [#]	DT [s]
100		7	1	0.8	14	1	0.6
200		15	1	0.6	11	1	0.8

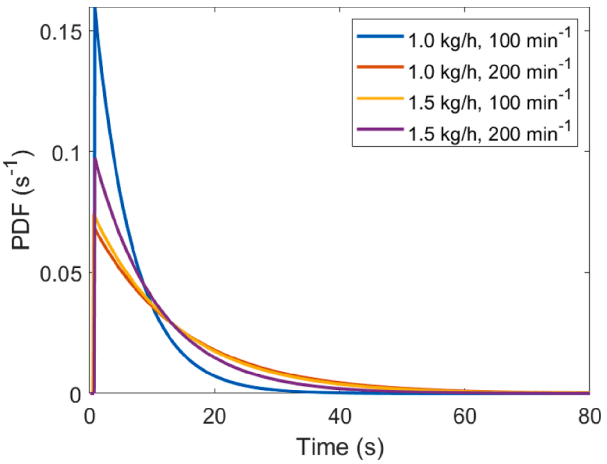

Fig. 8. Effect of CPPs on the RTD of the regranulation with CSTR models.

3.4. Integrated system

The integrated system's PDF was measured with impulse disturbances of colored powder blend into the hopper of the TSWG. Then the change of color in the product was measured only after the regranulation. Every CPP of the three-unit operations can affect the RTD of the integrated system. Therefore, all four CPPs should be considered in this RTD study. Examining previous levels would require an experimental design with 48 experiments, without repetition. Consequently, the number of experiments would be doubled, compared to the 20 experiments we have done by separating the unit operations. Furthermore, tracking the effect of individual CPPs would be more complicated if only the integrated system was measured.

Therefore, we calculated the three-step system's PDF with convolution and only measured four experiments with different CPPs. In the experiments, the parameters having the most significant effect on the RTD of the given unit operation were changed. Therefore, the screw rotational speed and the airflow were adjusted from 200 rpm to 400 rpm, and from 60 L/min to 120 L/min, respectively.

Comparing the calculated and measured RTD (Fig. 9) shows a proper correlation between the curves in the case of 120 L/min airflow, thereby proving the feasibility of the in silico method, which can be used for each combination of the investigated parameters. However, the correlation is better for the measured curve at 60 L/min airflow with the calculated 120 L/min curve than the calculated 60 L/min curve. The difference may derive from the different physical properties of the wet granule from the TSWG and the dried tracer granule. The dry and wet granules behave similarly at 120 L/min airflow due to the higher level of fluidization and faster drying of the granules. However, at 60 L/min the dried and wet granules may segregate creating a significant difference in the RTD.

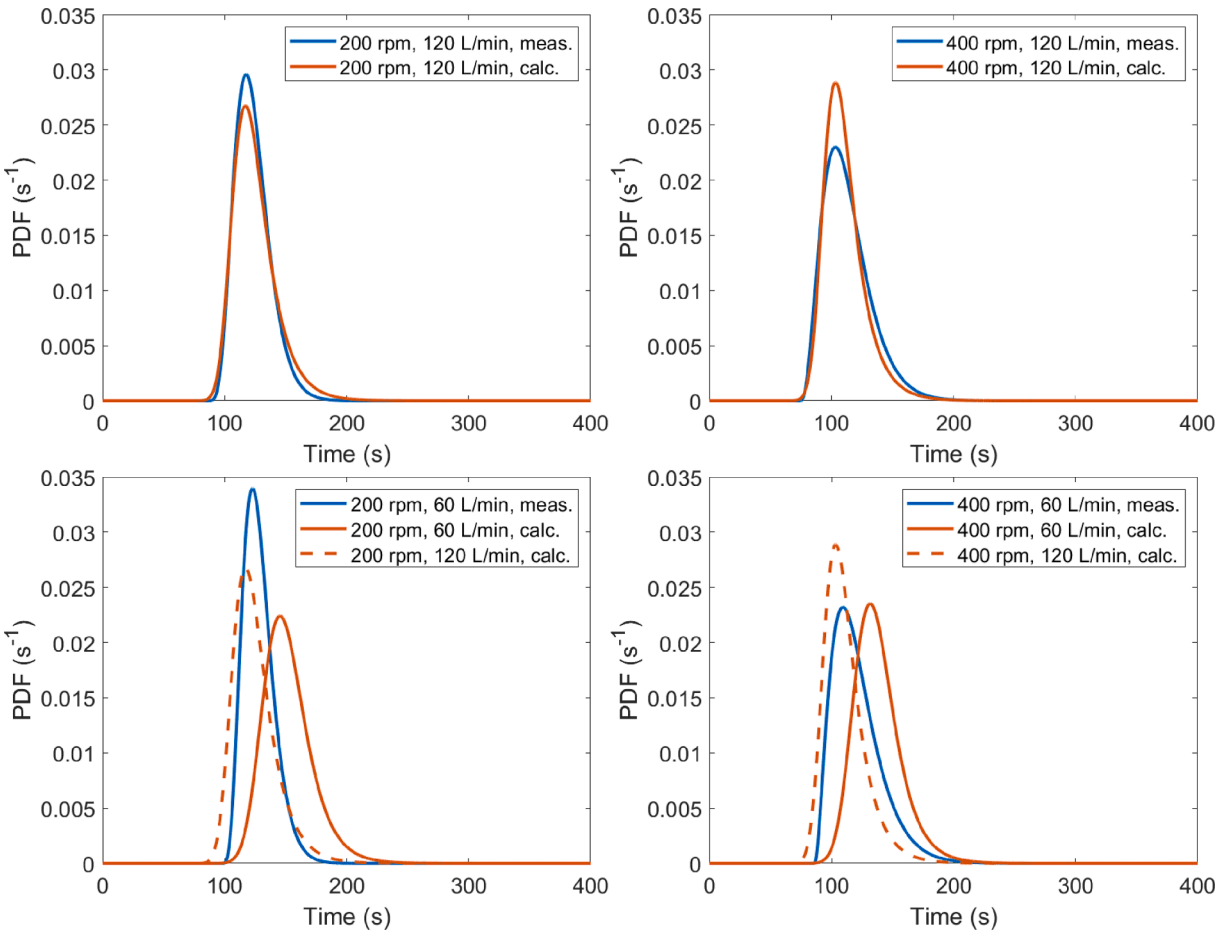

Fig. 9. Effect of screw rotational speed and airflow on the integrated system based on measurement and calculation.

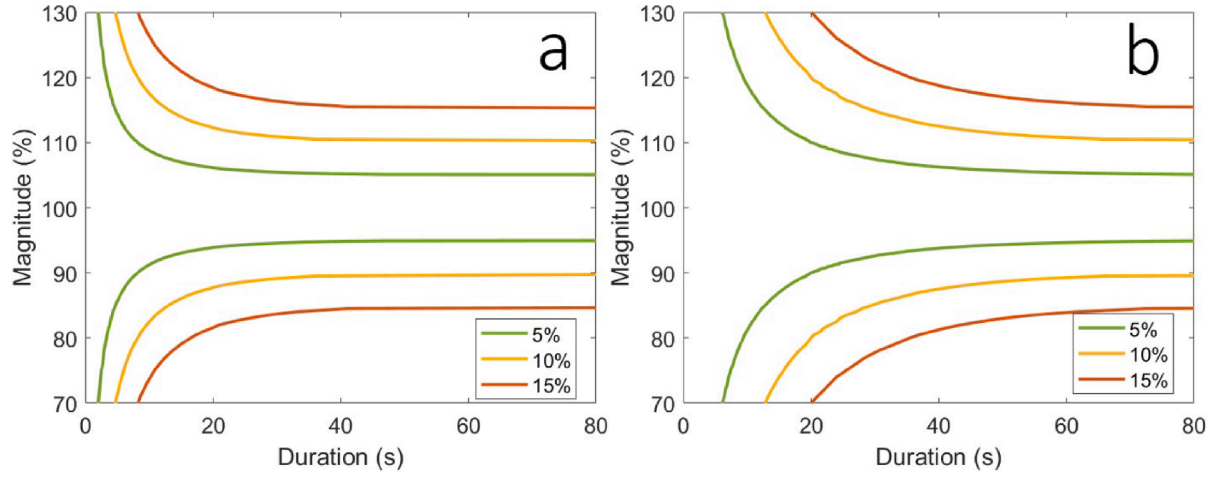

Fig. 10. Funnel plot of the TSWG for the powder blend (**a**) and funnel plot of the powder blend for the integrated system (**b**).

3.5. Application of RTD for the determination of control limits

RTD can be beneficial for developing a control limit-based control strategy with funnel plots and as a soft sensor-based prediction of output quality. Due to environmental effects, the feeding of input material is prone to disturbances, which can lead to insufficient content uniformity. These disturbances occur as the continuous feeder fails to keep the feeding setpoint for a short period of time.

Funnel plots place the maximum output error as the result of disturbances with known magnitude and duration. On selected error levels, the magnitude-duration pairs with the symmetrical negative magnitude-duration pairs form funnel-like curves, as the magnitude approaches the error level exponentially as the duration of the disturbance is increased.

The dampening effect of the consecutive processes is visible in the comparison of the funnel plot of the TSWG and the integrated process (Fig. 10). The mixing effect of the dryer and the mill significantly improves the product's content uniformity, compared to the TSWG. During

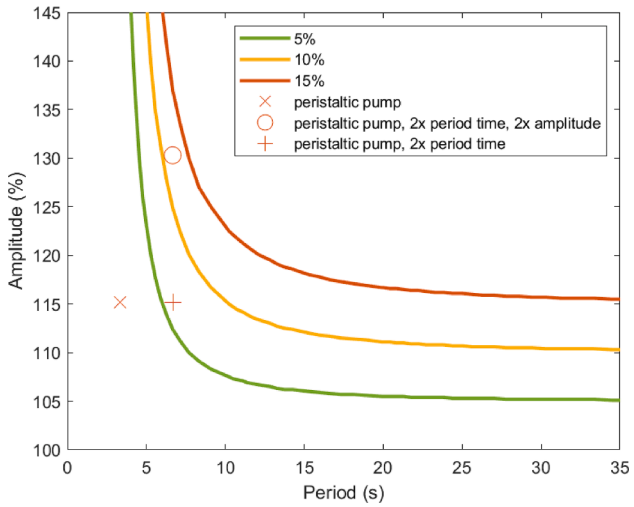

Fig. 11. Funnel plot based on the sine characteristic, with peristaltic pumps of various attributes placed on the plot.

process optimization, funnel plots can be used based on feeder characteristic measurements, further reducing the number of experiments and increasing the process understanding.

In previous research (Démuth et al., 2020), three different pump characteristics were measured. In this system, a syringe pump was used as it has the most consistent profile compared to the sine-like profile of the commonly used peristaltic pump. A different funnel plot was needed to address the feasibility of the peristaltic pump by using the amplitude and frequency of the sine curve (Fig. 11). This plot is one-sided but very similar to the funnel plot. The measured profile is dampened properly even with the narrowest RTD of the TSWG process (1.0 kg/h mass flow, 400 rpm screw rotation speed), however, longer period times (lower flow speed), or higher amplitude (smaller tube) can significantly increase the error.

In order to test the entire system, the inputs have to be considered together. The inputs can only be merged after the TSWG because of the different RTD in the granulator. After the TSWG, by dividing the calculated liquid change by the solid change, the L/S in time can be calculated. It can be used as the input for the dryer and the mill. For the solid input, the feeder characteristics of a Brabender and a MechaCAD type twin-screw gravimetric feeders were investigated based on a previous publication (Gyürkés et al., 2020). The integrated system reduced the fluctuations to acceptable levels with all setups, even with the narrowest PDFs. (Supplementary Fig. 2).

3.6. Validation of the soft sensor

The RTD can be used to predict concentration when it is convolved with material inputs. This is a powerful soft sensor as it only requires the RTD model and the measured feeding rate in time. Our developed method is independent of the investigated concentration. To validate the soft sensor, step disturbances were investigated by changing the rate of liquid flow rate by 15% for concentration change of CAR in the granule. Sampling was done by collecting the product in every 10 s for the duration of 4 s starting 50 s after the step disturbance. Powder flow was kept constant with gravimetric feeding. The 100 mg of the collected samples were measured with HPLC, with a resolution close to 2% relative error.

In the first experiment, a short step change was performed, and the liquid flow was reduced to the original level after 60 s. According to the funnel plot (Fig. 12a), a 15% amplitude change for the duration of 60 s would approach 15% deviance but would not reach it. Our measurements show similar results, where the short step change produced a peak-shaped response, with the concentration going as high as 115% (Fig. 12b), and the CAR content has reduced back to 100% after the

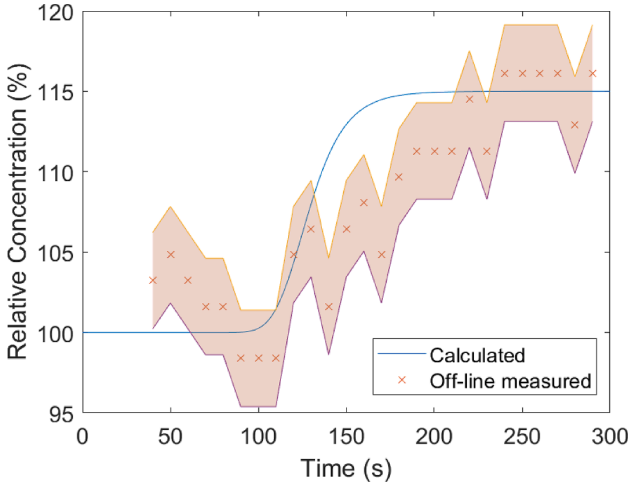

Fig. 13. Validation measurement with 15% step disturbance, with the red area showing the 3% relative error of the HPLC method. (For interpretation of the references to color in this figure legend, the reader is referred to the web version of this article.)

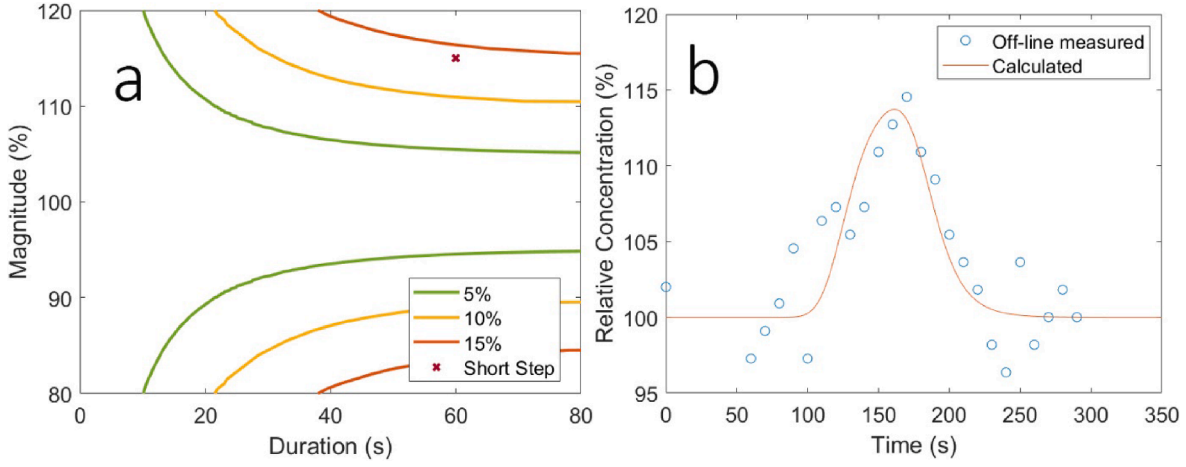

Fig. 12. Validation measurement with 15% short step disturbance for 60 s **a.,** placement of disturbance on funnel plot **b.,** HPLC-based concentration compared to the calculated curve.

peak, similarly to the predicted change in the concentration (RMSE = 2.5487%).

In the second experiment, the normal step change was measured. The digital twin calculation predicted the change adequately, as the time and shape of the step response were similar to the calculated curve (RMSE = 4.0008%) (Fig. 13).

These measurements ensure that the feeding rate of the inputs can be used as a soft sensor analytical method based on the RTD of the integrated system to predict the product concentration and content uniformity. These are traditionally time-consuming, destructive, and sometimes challenging procedures. In this formulation, the granulation liquid contains an extremely low dose of API, but the soft sensor-based prediction highly correlated with the HPLC measurements.

4. Conclusion

In this paper, we have successfully developed the dynamic model of a pharmaceutical powder to granule line and used the model as the basis for control limits, and an API concentration predicting soft sensor at ultra-low doses. We investigated the Residence Time Distribution of an integrated pharmaceutical line of three fully continuous unit operations by varying material inputs. The camera setup was a fast and easily applicable analytical approach for measuring colored material.

An approach is presented and validated for connecting individually measured models via convolution. The number of experiments to investigate the CPPs of the integrated system were halved by measuring single unit operations. Nevertheless, additional information was gathered by investigating the unit operations separately. The mass flow had no significant effect on the RTD of any unit operation in the analyzed range; therefore, fluctuations in mass flow do not affect the process stream. Significant factors for the RTD were identified for the processes of TSWG and drying, but integrated measurements has shown that the found effect was stronger for the tracer, due to physical differences in the system.

RTD has a crucial role in the control strategy. RTD has a dampening effect on the inputs, thereby filtering minor disturbances as the magnitude of the concentration change dampens. Furthermore, to ensure the measurement of impulse-like disturbances analytical sampling rate has to be adjusted to the width of the PDF. The precision of the feeding apparatus can be tested in silico at the feasibility point of view with the convolution of the feeder characteristics or by placing measured disturbances on funnel plots. Furthermore, when the production is disturbed, the time of waste collection can be precisely calculated with the RTD.

While the CU is one of the most important CQA, every unit operation has its dampening effect along the production line. Therefore, CU can be calculated from the input and the PDF of the integrated system. However, for some attributes, the RTD of single unit operation is critical as L/S remains constant after the TSWG and may cause disturbances, which other unit operations cannot compensate. The placement of analytical measurements and waste collection can be optimized with the help of connecting RTDs. By placing the waste separation closer to the end of the line, waste may increase due to the backmixing during unit operations. However, the same processes may reduce the magnitude of the disturbances to acceptable levels, therefore reducing waste. The same calculations were used to develop the soft sensor, which proved to be reliable even compared to HPLC measurements, with API content close to the HPLC measurement limit.

CRediT authorship contribution statement

Martin Gyürkés: Writing – original draft, Methodology, Investigation. **Lajos Madarász:** Investigation, Software. **Petra Záhonyi:** Investigation, Visualization. **Ákos Köte:** Software, Data curation. **Brigitta Nagy:** Data curation, Formal analysis. **Hajnalka Pataki:** Supervision, Validation. **Zsombor Kristóf Nagy:** Conceptualization, Validation. **András Domokos:** Methodology, Writing – review & editing. **Attila Farkas:** Conceptualization, Writing – review & editing.

Declaration of Competing Interest

The authors declare that they have no known competing financial interests or personal relationships that could have appeared to influence the work reported in this paper.

Acknowledgements

A. Farkas acknowledges the financial support received through the PREMIUM post-doctorate research program of the Hungarian Academy of Sciences, later Eötvös Loránd Research Network. This work was supported by OTKA grant FK-132133. This work was supported by the ÚNKP-21-3-II-BME-309 and ÚNKP-21-4-I-BME-329. New National Excellence Program of the Ministry for Innovation and Technology from the source of the National Research, Development and Innovation Fund. The research reported in this paper and carried out at BME has been supported by the National Laboratory of Artificial Intelligence funded by the NRDIO under the auspices of the Ministry for Innovation and Technology.

Appendix A. Supplementary material

Supplementary data to this article can be found online at https://doi.org/10.1016/j.ijpharm.2022.121950.

References

Adamo, A., Beingessner, R.L., Behnam, M., Chen, J., Jamison, T.F., Jensen, K.F., Monbaliu, J.-C.- M., Myerson, A.S., Revalor, E.M., Snead, D.R., Stelzer, T., Weeranoppanant, N., Wong, S.Y., Zhang, P., 2016. On-demand continuous-flow production of pharmaceuticals in a compact, reconfigurable system. Science 352 (6281), 61–67.

Allison, G., Cain, Y.T., Cooney, C., Garcia, T., Bizjak, T.G., Holte, O., Jagota, N., Komas, B., Korakianiti, E., Kourti, D., Madurawe, R., Morefield, E., Montgomery, F., Nasr, M., Randolph, W., Robert, J.L., Rudd, D., Zezza, D., 2015. Regulatory and quality considerations for continuous manufacturing May 20-21, 2014 continuous manufacturing symposium. J. Pharm. Sci. 104, 803–812. https://doi.org/10.1002/jps.24324.

Babu, M.P., Setty, Y.P., 2003. Residence Time Distribution of Solid in a Fluidized Bed. Can. J. Chem. Eng. 81, 118–123. https://doi.org/10.1002/cjce.5450810114.

Balogh, A., Domokos, A., Farkas, B., Farkas, A., Rapi, Z., Kiss, D., Nyiri, Z., Eke, Z., Szarka, G., Örkényi, R., Mátravölgyi, B., Faigl, F., Marosi, G., Nagy, Z.K., 2018. Continuous end-to-end production of solid drug dosage forms: Coupling flow synthesis and formulation by electrospinning. Chem. Eng. J. 350, 290–299. https://doi.org/10.1016/j.cej.2018.05.188.

Bhaskar, A., Singh, R., 2019. Residence Time Distribution (RTD)-Based Control System for Continuous Pharmaceutical Manufacturing Process. J. Pharm. Innov. 14 (4), 316–331.

Beke, Á.K., Gyürkés, M., Nagy, Z.K., Marosi, G., Farkas, A., 2021. Digital twin of low dosage continuous powder blending – Artificial neural networks and residence time distribution models. Eur. J. Pharm. Biopharm. 169, 64–77. https://doi.org/10.1016/j.ejpb.2021.09.006.

Bhalode, P., Tian, H., Gupta, S., Razavi, S.M., Roman-Ospino, A., Talebian, S., Singh, R., Scicolone, J.V., Muzzio, F.J., Ierapetritou, M., 2021. Using Residence time distribution in pharmaceutical solid dose manufacturing – a critical review. Int. J. Pharm. 610, 121248 https://doi.org/10.1016/j.ijpharm.2021.121248.

Chen, H., Diep, E., Langrish, T.A.G., Glasser, B.J., 2020. Continuous fluidized bed drying: Residence time distribution characterization and effluent moisture content prediction. AIChE J. 66 https://doi.org/10.1002/aic.16902.

Cole, K.P., Groh, J.M., Johnson, M.D., Burcham, C.L., Campbell, B.M., Diseroad, W.D., Heller, M.R., Howell, J.R., Kallman, N.J., Koenig, T.M., May, S.A., Miller, R.D., Mitchell, D., Myers, D.P., Myers, S.S., Phillips, J.L., Polster, C.S., White, T.D., Cashman, J., Hurley, D., Moylan, R., Sheehan, P., Spencer, R.D., Desmond, K., Desmond, P., Gowran, O., 2017. Kilogram-scale prexasertib monolactate monohydrate synthesis under continuous-flow CGMP conditions. Science 356 (6343), 1144–1150.

De Beer, T., Bodson, C., Dejaegher, B., Walczak, B., Vercruysse, P., Burggraeve, A., Lemos, A., Delattre, L., Vander Heyden, Y., Remon, J.P., Vervaet, C., Baeyens, W.R. G., 2008. Raman spectroscopy as a process analytical technology (PAT) tool for the in-line monitoring and understanding of a powder blending process. J. Pharm. Biomed. Anal. 48, 772–779. https://doi.org/10.1016/j.jpba.2008.07.023.

De Beer, T., Burggraeve, A., Fonteyne, M., Saerens, L., Remon, J.P., Vervaet, C., 2011. Near infrared and Raman spectroscopy for the in-process monitoring of

pharmaceutical production processes. Int. J. Pharm. 417, 32–47. https://doi.org/10.1016/j.ijpharm.2010.12.012.
Démuth, B., Fülöp, G., Kovács, M., Madarász, L., Ficzere, M., Köte, Á., Szabó, B., Nagy, B., Balogh, A., Csorba, K., Kaszás, G., Nagy, T., Bódis, A., Marosi, G., Nagy, Z.K., 2020. Continuous manufacturing of homogeneous ultralow-dose granules by twin-screw wet granulation, Period. Polytech. Chem. Eng. 64, 391–400. https://doi.org/10.3311/PPch.14972.
Domokos, A., Nagy, B., Gyürkés, M., Farkas, A., Tacsi, K., Pataki, H., Liu, Y.C., Balogh, A., Firth, P., Szilágyi, B., Marosi, G., Nagy, Z.K., Nagy, Z.K., 2020. End-to-end continuous manufacturing of conventional compressed tablets: From flow synthesis to tableting through integrated crystallization and filtration. Int. J. Pharm. 581, 119297 https://doi.org/10.1016/j.ijpharm.2020.119297.
Domokos, A., Nagy, B., Szilágyi, B., Marosi, G., Nagy, Z.K., 2021a. Integrated Continuous Pharmaceutical Technologies - A Review. Org. Process Res. Dev. 25, 721–739. https://doi.org/10.1021/acs.oprd.0c00504.
Domokos, A., Pusztai, É., Madarász, L., Nagy, B., Gyürkés, M., Farkas, A., Casian, T., Szilágyi, B., Kristóf, Z., 2021. Combination of PAT and mechanistic modeling tools in a fully continuous powder to granule line : Rapid and deep process understanding, 388 70–81. https://doi.org/10.1016/j.powtec.2021.04.059.
Dülle, M., Özcoban, H., Leopold, C.S., 2018. Investigations on the residence time distribution of a three-chamber feed frame with special focus on its geometric and parametric setups. Powder Technol. 331, 276–285. https://doi.org/10.1016/j.powtec.2018.03.019.
Engisch, W., Muzzio, F., 2016. Using Residence Time Distributions (RTDs) to Address the Traceability of Raw Materials in Continuous Pharmaceutical Manufacturing. J. Pharm. Innov. 11, 64–81. https://doi.org/10.1007/s12247-015-9238-1.
USD of H. and HS FDA, Guidance for Industry PAT — A Framework for Innovative Pharmaceutical Development, Manufacuring, and Quality Assurance, FDA Off. Doc. (2004) 16. https://doi.org/http://www.fda.gov/CDER/guidance/6419fnl.pdf.
US Food and Drug Administration, Draft Guidance for Industry - Quality Considerations for Continuous Manufacturing, (2019). [accessed 2021 Dec 13]. https://www.fda.gov/media/121314/download.
Furukawa, R., Singh, R., Ierapetritou, M., 2020. Effect of material properties on the residence time distribution (RTD) of a tablet press feed frame. Int. J. Pharm. 591, 119961 https://doi.org/10.1016/j.ijpharm.2020.119961.
Fülöp, G., Domokos, A., Galata, D., Szabó, E., Gyürkés, M., Szabó, B., Farkas, A., Madarász, L., Démuth, B., Lendér, T., Nagy, T., Kovács-Kiss, D., Van der Gucht, F., Marosi, G., Nagy, Z.K., 2021. Integrated twin-screw wet granulation, continuous vibrational fluid drying and milling: A fully continuous powder to granule line. Int. J. Pharm. 594, 120126.
Gao, Y., Vanarase, A., Muzzio, F., Ierapetritou, M., 2011. Characterizing continuous powder mixing using residence time distribution. Chem. Eng. Sci. 66, 417–425. https://doi.org/10.1016/j.ces.2010.10.045.
Gao, Y., Muzzio, F.J., Ierapetritou, M.G., 2012a. A review of the Residence Time Distribution (RTD) applications in solid unit operations. Powder Technol. 228, 416–423. https://doi.org/10.1016/j.powtec.2012.05.060.
Gao, Y., Muzzio, F.J., Ierapetritou, M.G., 2012b. Optimizing continuous powder mixing processes using periodic section modeling. Chem. Eng. Sci. 80, 70–80. https://doi.org/10.1016/j.ces.2012.05.037.
Gyürkés, M., Madarász, L., Köte, Á., Domokos, A., Mészáros, D., Beke, Á.K., Nagy, B., Marosi, G., Pataki, H., Nagy, Z.K., Farkas, A., 2020. Process design of continuous powder blending using residence time distribution and feeding models. Pharmaceutics. 12, 1–20. https://doi.org/10.3390/pharmaceutics12111119.
ICH, Q3C INTERNATIONAL COUNCIL FOR HARMONISATION OF TECHNICAL REQUIREMENTS FOR PHARMACEUTICALS FOR HUMAN USE ICH HARMONISED GUIDELINE IMPURITIES: GUIDELINE FOR RESIDUAL SOLVENTS Q3C(R6) Final version, (2016). [accessed 2021 Dec 13]. https://database.ich.org/sites/default/files/ICH_Q13_Step2_DraftGuideline_%202021_0727.pdf.
Ierapetritou, M., Roman-Ospino, A., Moghtadernejad, S., Cappuyns, P., Futran, M., Van Assche, I., Sebastian Escotet-Espinoza, M., Muzzio, F., Oka, S., Schäfer, E., Wang, Y., 2018. Effect of tracer material properties on the residence time distribution (RTD) of continuous powder blending operations. Part I of II: Experimental evaluation. Powder Technol. 342, 744–763. https://doi.org/10.1016/j.powtec.2018.10.040.
J. M. Juran, Juran on Quality by Design (The New Steps for Planning Quality into Goods and Services), 1992, ISBN: 9780029166833.
Karttunen, A.P., Hörmann, T.R., De Leersnyder, F., Ketolainen, J., De Beer, T., Hsiao, W. K., Korhonen, O., 2019. Measurement of residence time distributions and material tracking on three continuous manufacturing lines. Int. J. Pharm. 563, 184–197. https://doi.org/10.1016/j.ijpharm.2019.03.058.
Karttunen, A.P., Poms, J., Sacher, S., Sparén, A., Ruiz Samblás, C., Fransson, M., Martin De Juan, L., Remmelgas, J., Wikström, H., Hsiao, W.K., Folestad, S., Korhonen, O., Abrahmsén-Alami, S., Tajarobi, P., 2020. Robustness of a continuous direct compression line against disturbances in feeding. Int. J. Pharm. 574, 118882 https://doi.org/10.1016/j.ijpharm.2019.118882.
Kotamarthy, L., Ramachandran, R., 2021. Mechanistic understanding of the effects of process and design parameters on the mixing dynamics in continuous twin-screw granulation. Powder Technol. 390, 73–85. https://doi.org/10.1016/j.powtec.2021.05.071.
Kreimer, M., Aigner, I., Lepek, D., Khinast, J., 2018. Continuous Drying of Pharmaceutical Powders Using a Twin-Screw Extruder. Org. Process Res. Dev. 22, 813–823. https://doi.org/10.1021/acs.oprd.8b00087.
Kruisz, J., Rehrl, J., Sacher, S., Aigner, I., Horn, M., Khinast, J.G., 2017. RTD modeling of a continuous dry granulation process for process control and materials diversion. Int. J. Pharm. 528, 334–344. https://doi.org/10.1016/j.ijpharm.2017.06.001.
Kumar, A., Vercruysse, J., Vanhoorne, V., Toiviainen, M., Panouillot, P.E., Juuti, M., Vervaet, C., Remon, J.P., Gernaey, K.V., De Beer, T., Nopens, I., 2015. Conceptual framework for model-based analysis of residence time distribution in twin-screw granulation. Eur. J. Pharm. Sci. 71, 25–34. https://doi.org/10.1016/j.ejps.2015.02.004.
Kumar, A., Alakarjula, M., Vanhoorne, V., Toiviainen, M., De Leersnyder, F., Vercruysse, J., Juuti, M., Ketolainen, J., Vervaet, C., Remon, J.P., Gernaey, K.V., De Beer, T., Nopens, I., 2016. Linking granulation performance with residence time and granulation liquid distributions in twin-screw granulation: An experimental investigation. Eur. J. Pharm. Sci. 90, 25–37. https://doi.org/10.1016/j.ejps.2015.12.021.
Laske, S., Paudel, A., Scheibelhofer, O., Sacher, S., Hoermann, T., Khinast, J., Kelly, A., Rantannen, J., Korhonen, O., Stauffer, F., De Leersnyder, F., De Beer, T., Mantanus, J., Chavez, P.F., Thoorens, B., Ghiotti, P., Schubert, M., Tajarobi, P., Haeffler, G., Lakio, S., Fransson, M., Sparen, A., Abrahmsen-Alami, S., Folestad, S., Funke, A., Backx, I., Kavsek, B., Kjell, F., Michaelis, M., Page, T., Palmer, J., Schaepman, A., Sekulic, S., Hammond, S., Braun, B., Colegrove, B., 2017. A Review of PAT Strategies in Secondary Solid Oral Dosage Manufacturing of Small Molecules. J. Pharm. Sci. 106, 667–712. https://doi.org/10.1016/j.xphs.2016.11.011.
Lee, S.L., Connor, T.F.O., Yang, X., Cruz, C.N., Yu, L.X., Woodcock, J., 2015. Modernizing Pharmaceutical Manufacturing : from Batch to Continuous. Production. https://doi.org/10.1007/s12247-015-9215-8.
Mangal, H., Kleinebudde, P., 2017. Experimental determination of residence time distribution in continuous dry granulation. Int. J. Pharm. 524, 91–100. https://doi.org/10.1016/j.ijpharm.2017.03.085.
Martinetz, M.C., Karttunen, A.P., Sacher, S., Wahl, P., Ketolainen, J., Khinast, J.G., Korhonen, O., 2018. RTD-based material tracking in a fully-continuous dry granulation tableting line. Int. J. Pharm. 547, 469–479. https://doi.org/10.1016/j.ijpharm.2018.06.011.
Mascia, S., Heider, P.L., Zhang, H., Lakerveld, R., Benyahia, B., Barton, P.I., Braatz, R.D., Cooney, C.L., Evans, J.M.B., Jamison, T.F., Jensen, K.F., Myerson, A.S., Trout, B.L., 2013. End-to-End Continuous Manufacturing of Pharmaceuticals: Integrated Synthesis, Purification, and Final Dosage Formation, Angew. Chemie. 125, 12585–12589. https://doi.org/10.1002/ange.201305429.
Muzzio, F., Oka, S., 2017. Using residence time distribution to understand continuous blending. Powder Bulk Eng.
Nauman, E.B., 2008. Residence time theory. Ind. Eng. Chem. Res. 47, 3752–3766. https://doi.org/10.1021/ie071635a.
Oka, S., Van Assche, I., Futran, M., Muzzio, F., Escotet-Espinoza, M.S., Wang, Z., Roman-Ospino, A., Wang, Y., Schäfer, E., Cappuyns, P., Moghtadernejad, S., Ierapetritou, M., 2018. Effect of material properties on the residence time distribution (RTD) characterization of powder blending unit operations. Part II of II: Application of models, Powder Technol. 344, 525–544. https://doi.org/10.1016/j.powtec.2018.12.051.
Pauli, V., Kleinebudde, P., Krumme, M., 2020. Predictive model-based process start-up in pharmaceutical continuous granulation and drying. Pharmaceutics. 12, 1–11. https://doi.org/10.3390/pharmaceutics12010067.
Plath, T., Korte, C., Sivanesapillai, R., Weinhart, T., 2021. Parametric study of residence time distributions and granulation kinetics as a basis for process modeling of twin-screw wet granulation. Pharmaceutics. 13 (5), 645.
K. Plumb, Continuous Processing in the Pharmaceutical Industry: Changing the Mind Set. Chem. Eng. Res. Des. 83 (2005), 730–738. dx.doi.org/10.1205/cherd.04359.
Poechlauer, P., Manley, J., Broxterman, R., Gregertsen, B., Ridemark, M., 2012. Continuous processing in the manufacture of active pharmaceutical ingredients and finished dosage forms: An industry perspective. Org. Process Res. Dev. 16, 1586–1590. https://doi.org/10.1021/op300159y.
Rahimi, S.K., Paul, S., Sun, C.C., Zhang, F., 2020. The role of the screw profile on granular structure and mixing efficiency of a high-dose hydrophobic drug formulation during twin screw wet granulation. Int. J. Pharm. 575, 118958 https://doi.org/10.1016/j.ijpharm.2019.118958.
Rehrl, J., Karttunen, A.P., Nicolaï, N., Hörmann, T., Horn, M., Korhonen, O., Nopens, I., De Beer, T., Khinast, J.G., 2018. Control of three different continuous pharmaceutical manufacturing processes: Use of soft sensors. Int. J. Pharm. 543, 60–72. https://doi.org/10.1016/j.ijpharm.2018.03.027.
Roggo, Y., Pauli, V., Jelsch, M., Pellegatti, L., Elbaz, F., Ensslin, S., Kleinebudde, P., Krumme, M., 2020. Continuous manufacturing process monitoring of pharmaceutical solid dosage form: A case study. J. Pharm. Biomed. Anal. 179, 112971 https://doi.org/10.1016/j.jpba.2019.112971.
Schaber, S.D., Gerogiorgis, D.I., Ramachandran, R., Evans, J.M.B., Barton, P.I., Trout, B. L., 2011. Economic Analysis of Integrated Continuous and Batch Pharmaceutical Manufacturing : A Case Study. Ind. Eng. Chem. Res. 50 (17), 10083–10092. https://doi.org/10.1021/ie2006752.
Silva, A.F., Vercruysse, J., Vervaet, C., Remon, J.P., Lopes, J.A., De Beer, T., Sarraguça, M.C., 2018. Process monitoring and evaluation of a continuous pharmaceutical twin-screw granulation and drying process using multivariate data analysis. Eur. J. Pharm. Biopharm. 128, 36–47. https://doi.org/10.1016/j.ejpb.2018.04.011.
Simon, L.L., Pataki, H., Marosi, G., Meemken, F., Hungerbühler, K., Baiker, A., Tummala, S., Glennon, B., Kuentz, M., Steele, G., Kramer, H.J.M., Rydzak, J.W., Chen, Z., Morris, J., Kjell, F., Singh, R., Gani, R., Gernaey, K.V., Louhi-Kultanen, M., Oreilly, J., Sandler, N., Antikainen, O., Yliruusi, J., Frohberg, P., Ulrich, J., Braatz, R. D., Leyssens, T., Von Stosch, M., Oliveira, R., Tan, R.B.H., Wu, H., Khan, M., Ogrady, D., Pandey, A., Westra, R., Delle-Case, E., Pape, D., Angelosante, D., Maret, Y., Steiger, O., Lenner, M., Abbou-Oucherif, K., Nagy, Z.K., Litster, J.D., Kamaraju, V.K., Sen Chiu, M., 2015. Assessment of recent process analytical technology (PAT) trends: A multiauthor review. Org. Process Res. Dev. 19, 3–62. https://doi.org/10.1021/op500261y.

Tanimura, S., Singh, R., Román-Ospino, A.D., Ierapetritou, M., 2021. Residence time distribution modelling and in line monitoring of drug concentration in a tablet press feed frame containing dead zones. Int. J. Pharm. 592, 1–13. https://doi.org/10.1016/j.ijpharm.2020.120048.

Tian, G., Koolivand, A., Gu, Z., Orella, M., Shaw, R., O'Connor, T.F., 2021. Development of an RTD-Based Flowsheet Modeling Framework for the Assessment of In-Process Control Strategies. AAPS PharmSciTech. 22, 1–10. https://doi.org/10.1208/s12249-020-01913-8.

Wahl, P.R., Hörl, G., Kaiser, D., Sacher, S., Rupp, C.h., Shlieout, G., Breitenbach, J., Koscher, G., Khinast, J.G., 2018. In-Line Measurement of Residence Time Distribution in Melt Extrusion via Video Analysis. Polym. Eng. Sci. 58 (2), 170–179. https://doi.org/10.1002/pen.24544.

Wesholowski, J., Berghaus, A., Thommes, M., 2018. Investigations concerning the residence time distribution of twin-screw-extrusion processes as indicator for inherent mixing. Pharmaceutics. 10 (4), 207.

Wesholowski, J., Podhaisky, H., Thommes, M., 2019. Comparison of residence time models for pharmaceutical twin-screw-extrusion processes. Powder Technol. 341, 85–93. https://doi.org/10.1016/j.powtec.2018.02.054.